

Preparation and performance of a novel multifunctional plasma electrolytic oxidation composite coating formed on magnesium alloy

Jie Guo · Liping Wang · S. C. Wang ·
J. Liang · Qunji Xue · Fengyuan Yan

Received: 5 November 2008 / Accepted: 21 January 2009 / Published online: 18 February 2009
© Springer Science+Business Media, LLC 2009

Abstract Plasma electrolytic oxidation (PEO) in an alkaline phosphate electrolyte was used to produce a novel multifunctional polytetrafluoroethylene (PTFE)-containing oxide composite coatings on AM60B magnesium alloys. The composition and microstructure of the PTFE-containing PEO coatings were analyzed by X-ray photoelectron spectroscopy (XPS), X-ray diffraction (XRD), and scanning electron microscope (SEM). The electrochemical corrosion behavior, tribological properties, and wetting properties of the PTFE-containing PEO composite coatings were evaluated using potentiodynamic polarization measurements, a reciprocating ball-on-disk tribometer, and a contact angle meter, respectively. Results show that the PTFE-containing PEO composite coatings exhibited superior corrosion resistance, excellent self-lubricating property, and better hydrophobic property when compared with pure PEO coatings, and will be the attractive advanced materials for a wide range of functional applications.

J. Guo · L. Wang (✉) · Q. Xue · F. Yan
State Key Laboratory of Solid Lubrication, Lanzhou Institute
of Chemical Physics, Chinese Academy of Sciences,
Lanzhou 730000, People's Republic of China
e-mail: lpwang@lzb.ac.cn

J. Guo
Graduate School of Chinese Academy of Sciences,
Beijing 10039, People's Republic of China

S. C. Wang
National Centre for Advanced Tribology at Southampton
(nCATS), School of Engineering Sciences, University
of Southampton, Southampton SO17 1BJ, UK

J. Liang
GKSS-Research Center Geesthacht GmbH, Geesthacht 21502,
Germany

Introduction

Due to a unique combination of high strength-to-weight ratio, high dimensional stability, good machining and recycling ability, magnesium and its alloys are of interest in a wide range of industries, e.g. the automotive, aerospace, and communication fields [1]. Unfortunately, magnesium and its alloys have two great weaknesses, namely, their vulnerability to corrosion and wear [2]. These disadvantages strongly restrict the widespread applications of magnesium and its alloys, especially in some harsh service environments [3].

Currently, industrial application of magnesium alloys is limited to the static component field. However, in certain applications, magnesium alloys are subjected to sliding motion including automotive brakes, guide bars, bearing plates, seat supports, and engine components (piston and cylinder brakes). Sliding wear is also an important consideration in material processing by rolling, extrusion, forging, etc. Magnesium alloys in general, exhibit very poor tribological performance under unlubricated wear conditions resulting in severe seizing (seizing and wear). A more widespread use of magnesium alloys in the automotive industry demands powerful functional surface coatings to ensure better tribological property, as well as satisfying anticorrosion performance [4–7].

Plasma electrolytic oxidation (PEO) [8–12] which is a new and effective surface treatment technique developed from traditional anodic oxidation has been used for surface modification of Mg alloys and some significant results have been reported [9, 13–16]. PEO process could provide Mg alloys with thick, hard ceramic-like oxide coatings composed of outer porous layer and inner barrier layer [17, 18], and this ceramic-like coating can improve the corrosion resistance and antiwear abilities. However, the unavoidable porous

structures in the sintered ceramic-like PEO coatings decrease the corrosion resistance [19]. Furthermore, although PEO coatings improve the wear resistance of Mg alloy, they have higher friction coefficient than Mg alloys [20]. These disadvantages still restrict the potential applications of Mg alloys. Thus, the application of composite PEO coatings with a unique combination of high strength, better corrosion resistance, superior self-lubrication, and antiwear properties on Mg alloys would be attractive advanced coatings for a wide range of functional applications.

Polytetrafluoroethylene (PTFE) have been used successfully in many industries because of its many advantages such as nonstick, higher dry lubricity, lower friction, chemical inertness, hydrophobic, good wear, and good corrosion resistance properties. [21]. In this article, we have developed a method to introduce PTFE nanoparticles into the PEO coatings to combine their advantages together and improve the overall properties of the PEO coatings. To the best of our knowledge, this is the first report on the fabrication of such multifunctional PEO composite coatings formed on Mg alloys with superior self-lubrication, hydrophobic, and anticorrosion properties.

Experimental

Fabrication of PEO composite coatings on Mg alloys

Rectangular coupons ($20 \times 36 \times 2 \text{ mm}^3$) of AM60B magnesium alloy (mass fraction: 5.6%–6.4% Al, 0.26%–0.4% Mn, $\leq 0.2\%$ Zn, and Mg balance) was used as the substrate for depositing PEO coatings. Prior to PEO treatment, the substrates were ground and polished with SiC abrasive paper to achieve a surface finish of $R_a \approx 0.18 \mu\text{m}$ and then degreased in acetone. Dispersed PTFE nanoparticles suspension (10 wt%) was used as the additive in the alkaline phosphate electrolyte to prepare the PTFE-containing PEO coatings on Mg alloys. It is well known that surfactants cannot only improve the stability of a suspension by increasing the wettability and surface charge of suspended particles but also enhance the electrostatic adsorption of suspended particles on an anode surface by increasing their net positive charge. In this case, nonionic-surfactant (octylphenol polyoxyethylene ether, with the addition of 1–2 vol.% in dispersed PTFE suspension) and anionic surfactants (sodium dodecyl sulfonate, with the addition of 2–4 vol.% in dispersed PTFE suspension) were used for nano PTFE particles dispersion and surface charge adjustment.

The alkaline phosphate electrolyte was prepared from solution of sodium phosphate (10.0 g/L) in distilled water with the addition of potassium hydroxide (1.0 g/L) to adjust the pH and conductivity. The plasma electrolytic oxidation

processes were carried out in the alkaline phosphate electrolyte without and with the addition of 3 vol.% PTFE nanoparticles suspension (10 wt%), using a bipolar pulsed electrical source (Institute of Low Energy Nuclear Physics, Beijing Normal University, China). The electrical source provided the voltage and current waveforms as described in Ref. [22]. The electrical parameters were fixed as follows: frequency = 150 Hz, the positive pulse = 1.0 ms, the negative pulse = 1.5 ms, and duty cycle = 37.5%. The Mg alloy sample and the wall of the stainless steel container were used as the anode and the cathode, respectively. The voltages of the positive pulse cycle and the negative pulse cycle were controlled so as to maintain constant current density at 6.0 A/dm^2 (positive current density is equal to negative current density). The final voltage was kept at approximately 500 V. During the PEO process, the temperature of the electrolytes was always maintained within the range 25–30 °C by a mechanical stirrer in solution and a water cooling system. The treatment times were set at 5 min for the samples oxidized in alkaline phosphate electrolyte without and with PTFE nanoparticles, respectively. After the PEO treatment, the coated samples were rinsed thoroughly in water and dried in warm air.

Microstructure characterization

The Zeta potential of the modified nano PTFE particles added in the alkaline phosphate electrolyte was measured by a nanoparticle size analyzer (Zetasizer Nano ZS ZEN 3600, Malvern, UK). The size and morphology of these particles were observed by a JEOL JEM-1200EX transmission electron microscope (TEM).

A JEOL JSM-5600LV scanning electron microscope (SEM) was used to observe the surface and cross-section morphologies of the oxide coatings. The XPS analyses of the oxide coatings were performed on a PHI-5702 multifunctional X-ray photoelectron spectroscope, using Al-K α radiation (photon energy 1476.6 eV) as the excitation source. The binding energy of C1s (284.8 eV) was used as the reference. The phase composition of the oxide coatings was studied by X-ray diffraction (XRD, Philips X' Pert Pro MPD X-ray diffractometer), using Cu-K α radiation as the excitation source at a grazing angle of 2°.

Corrosion resistance, tribological, and hydrophobic properties evaluations

The electrochemical measurements were carried out in a three-electrode cell. The Mg alloys samples coated with PEO coating was used as a working electrode. A platinum plate and saturated calomel electrode (SCE) were used as counter and reference electrode, respectively. Measurements were performed in 3.5 wt% NaCl solutions at a

temperature of 20 °C using a CHI760B potentiostat/galvanostat system. Scan was conducted with a constant rate of 10 mV/s. Potentiodynamic anodic polarization curves were established and the corrosion potential (E_{corr}) and corrosion current density (i_{corr}) were determined using the Tafel extrapolation method.

The friction and wear properties of the uncoated Mg alloy, the PEO coating and PTFE-containing PEO coatings were evaluated on a reciprocating ball-on-disk UMT-2MT tribometer (Center for Tribology, California, USA). Our previous studies shown that wear life of the 5 min (oxidation time) PEO coatings is short [20], so in this case, the 30 min (oxidation time) PEO coatings which were prepared under the same conditions were chosen for friction and wear tests. A AISI52100 steel ball (diameter 3 mm, hardness HRC 62 ~ 63, surface roughness Ra about 0.01 μm) was used as the counter body and its chemical compositions is C (0.95–1.05 wt%), Si (0.15–0.35 wt%), Mn (0.2–0.4 wt%), Cr (1.30–1.65 wt%), and Fe (balance). All the wear tests were performed using a load of 2 N, a sliding frequency of 5 Hz, and sliding amplitude of 5 mm at room temperature. The friction coefficient and sliding time were recorded automatically during the tests.

Sessile water droplet contact angle (CA) values were acquired using a contact angle meter (CA-A type, Kyowa Scientific Company, Ltd., Japan) at ambient temperature. The average CA values were obtained by measuring the sample at five different positions, and the images were captured with a digital camera (Panasonic, Ltd., Japan).

Results and discussion

Characteristics of PTFE nanoparticles

It is well known that nanoparticles tend to agglomerate in an electrolyte due to high surface free energy and high ionic strength of the electrolyte [23]. The agglomeration makes the co-deposition of the nanoparticle relatively difficult. It has been widely reported that surface modification of these particles, especially the addition of surfactants, can overcome this problem significantly [24–26]. The Zeta potentials of the modified PTFE nanoparticles added in the alkaline phosphate electrolyte immediately (a) and after 24 h (b) were measured, respectively. The Zeta potential of the PTFE particles was about -6 mV, but after 24 h it changed to about -3 mV. From the bright field TEM image of the treated PTFE nanoparticles (Fig. 1) it can be seen that the particles with diameters in the range of 170–270 nm were wrapped by the layers of surfactants and uniformly dispersed in water with slight aggregation. The composite surfactants containing nonionic and anionic surfactants improved the wettability and stability of the suspension by

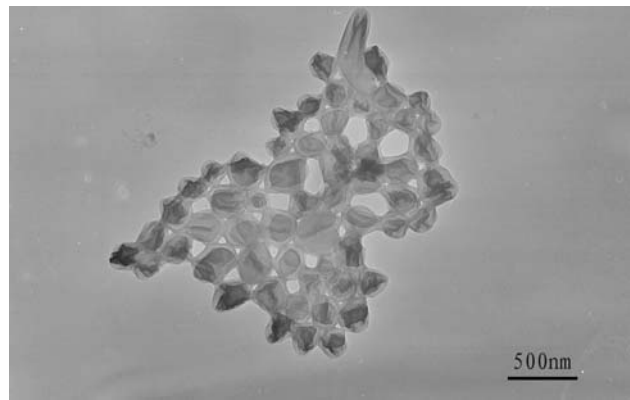


Fig. 1 Bright field TEM image of the treated PTFE nanoparticles

changing the surface polarity of the inert PTFE nanoparticles. Furthermore, the anionic surfactants increased the negative charge (known as the Zeta potential) of the PTFE nanoparticles, which will be useful for the electrophoresis and subsequent electrostatic adsorption of PTFE particles towards Mg alloy anodes and for the co-deposition of PTFE particles in PEO coatings [27].

Characteristics of PTFE-containing PEO coatings

Figure 2 shows the development of the positive voltage of the anodization as a function of time of the plasma electrolytic oxidation processes in alkaline phosphate electrolyte without and with the addition of PTFE particles using a constant current density mode. It can be seen that the variation of the positive voltage is similar for the two solutions, but the work and final voltage for the solution containing PTFE particles is slightly smaller than that without PTFE particles during PEO process. The chemical compositions of

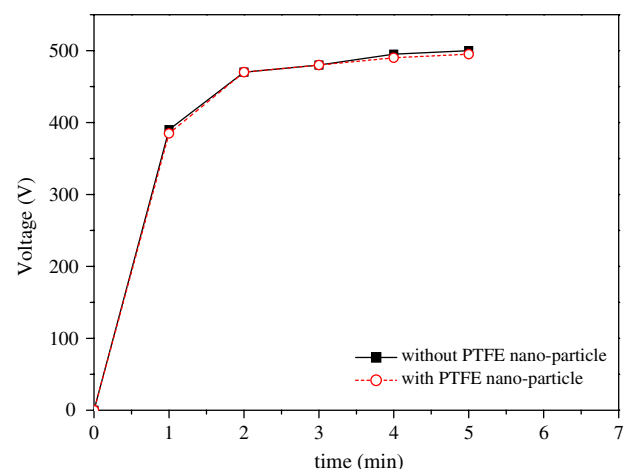


Fig. 2 Variation of positive voltage in alkaline phosphate electrolyte without and with the addition of PTFE particles

the PEO coatings formed in alkaline phosphate electrolyte with and without the addition of PTFE nanoparticles were determined by XPS analyses. The XPS survey spectra and

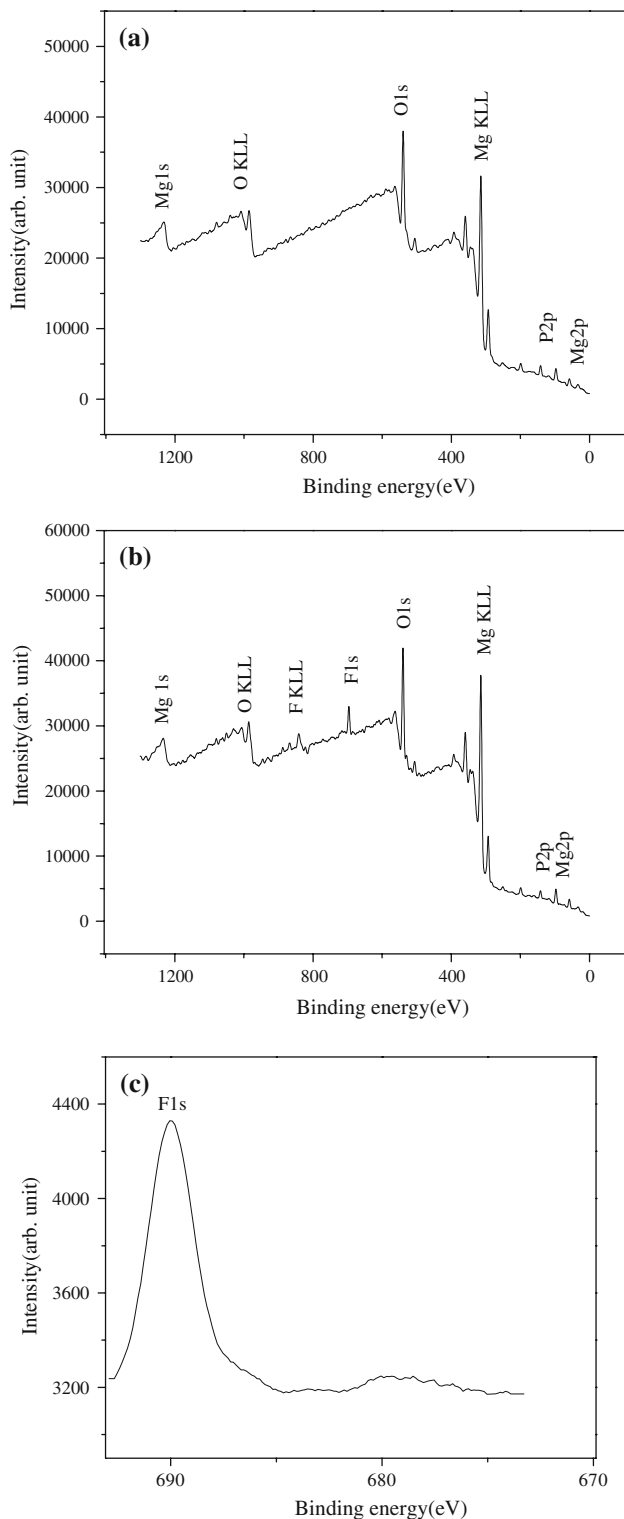


Fig. 3 XPS survey spectra of **a** the PEO coating and **b** the PTFE-containing PEO coating, **c** Typical XPS specific spectrum of F1s for the PTFE-containing PEO coatings

specific spectrum of F1s of the oxide coatings are shown in Fig. 3a, b, and c, respectively. It can be seen from Fig. 3a that the pure PEO oxide coatings formed in alkaline phosphate electrolyte contain mainly O, Mg, and P. For the PEO oxide coatings formed in electrolyte with the addition of PTFE nanoparticles, there is an evident peak of F1s, as well as the above O, Mg, and P elements (Fig. 3b), indicating that the fluorine element which is the component of the PTFE nanoparticles incorporated into the oxide coatings during the PEO process. Figure 3c demonstrates the specific spectrum of F1s taken from the composite oxide coatings formed in electrolyte with addition of PTFE nanoparticles. It can be seen that the spectrum has only one peak at 690.0 eV corresponding to CF₂ group ($\begin{matrix} \text{F} & \text{F} \\ | & | \\ -\text{C} & - & \text{C}- \\ | & | \\ \text{F} & \text{F} \end{matrix}$), which constitutes the basic unit in the structure of PTFE. It is inferred that the PTFE nanoparticles incorporated into the PEO oxide coatings exist in the form of PTFE [28].

X-ray diffraction (XRD) analyses were used to further investigate the changes in composition of PEO coatings before and after the addition of PTFE nanoparticles into the alkaline phosphate electrolyte. The spectrum of the PEO film labeled A in Fig. 4 shows the peaks corresponding to MgO, Mg, and MgAl₂O₄, respectively. The spectrum of the PEO film formed with addition of PTFE nanoparticles (spectrum B in Fig. 4) shows a new peak at 2θ around 18°, indicating the existence of an integrated PTFE phase. This clearly demonstrated that PTFE particles were effectively incorporated in the PEO coatings, which is in agreement with the results of XPS analyses.

Figures 5, 6 show the surface and cross-section morphologies of pure PEO coating and PTFE-containing PEO composite coatings, respectively. As can be seen, micropores and cracks are found to be existed on the surface of the

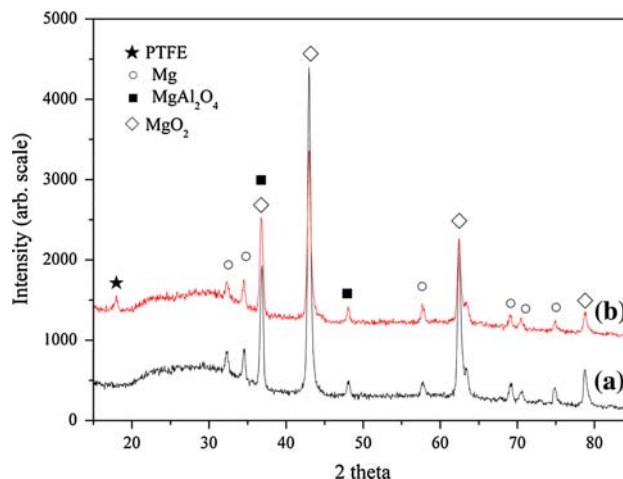


Fig. 4 XRD patterns of PEO coatings formed in an alkaline phosphate bath (a) without and (b) with addition of PTFE nanoparticles

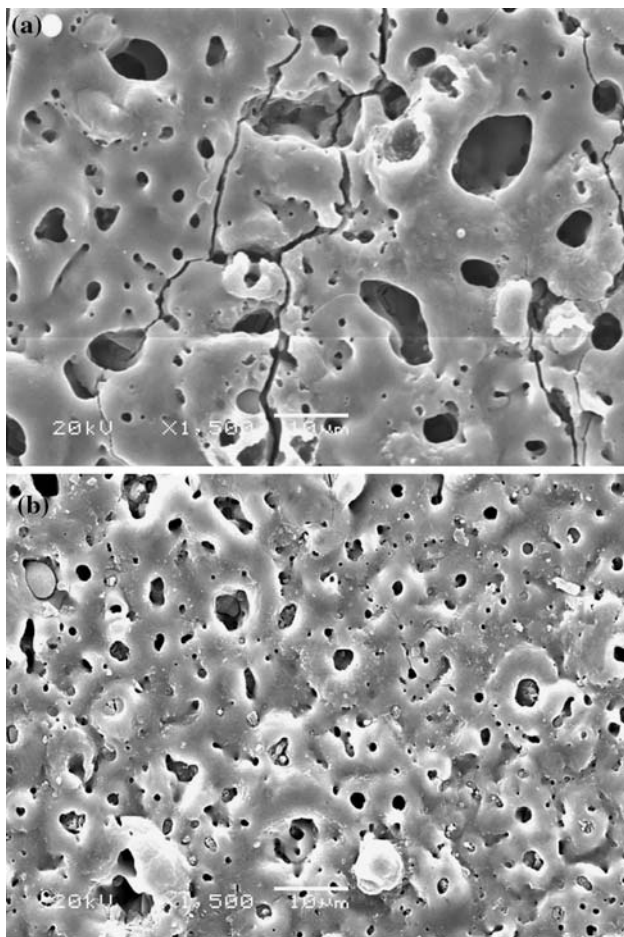


Fig. 5 SEM surface morphologies for **a** PEO coating and **b** PTFE-containing PEO coatings

pure PEO coating (Fig. 5a). The diameter of the micropores ranges from a few to more than ten micrometers. The cracks are relatively wide and long, even going through the micropores. The pores were formed by the molten oxide and gas bubbles thrown out of microarc discharge channels, while the microcracks resulted from the thermal stress due to the rapid solidification of the molten oxide in the relatively cold electrolyte [9, 29, 30]. As shown in the cross-sectional morphology (Fig. 6a) the PEO coating with thickness of about 15 μm grown on the magnesium alloy is composed of an outer porous layer and an inner barrier layer. There are also many pores and microcracks in the cross-sectional morphology. Compared with the inner layer, the outer layer is more porous which would permit more corrosive medium to get through and reach the magnesium substrate, and decrease the corrosion resistance of PEO coatings on magnesium alloy substrates [12]. In contrast, the micropores on the surface of the PTFE-containing composite coatings are small and relatively homogeneous (Fig. 5b). In addition, the cracks that can be easily found on the surface of pure PEO coatings can hardly be found on the surface of

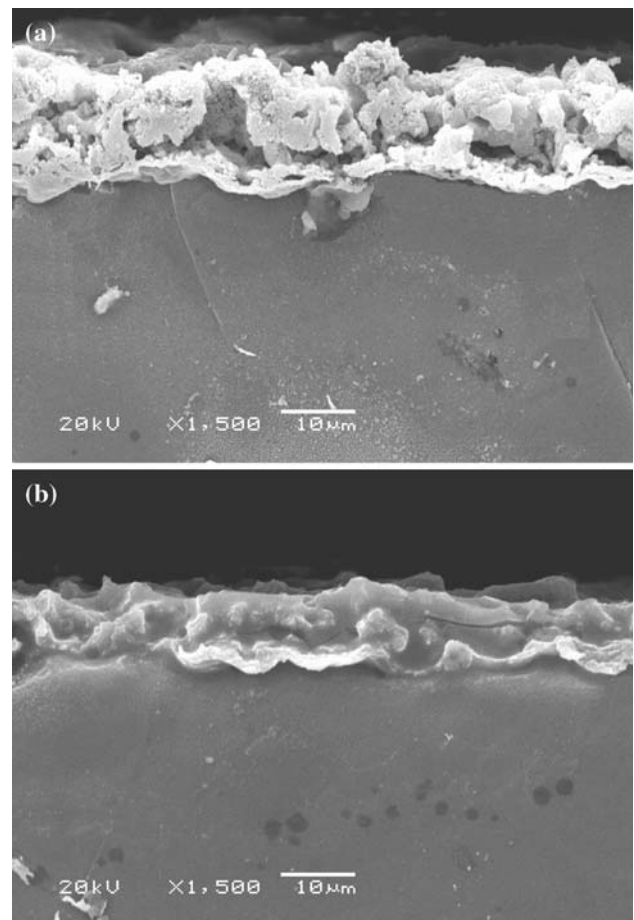


Fig. 6 SEM cross-sectional morphologies for **a** PEO coating and **b** PTFE-containing PEO coating

PTFE-containing PEO coatings. In the cross-sectional morphology of PTFE-containing PEO coatings (Fig. 6b), it can be clearly observed that the composite oxide coating with a thickness about 13 μm is dense without through-going pores or defects. The PTFE-containing PEO coating appeared to be well bonded with the substrate and the pores and microcracks can hardly be found in the outer layer. As a result, the corrosive medium can not get through the oxide coatings so easily. During the PEO process, the PTFE nanoparticles with negative Zeta potential in the electrolyte could move towards anode (Mg alloy) under the electric field force and then co-deposit on the surface of the Mg alloy. These particles could be partly filled in the micropores and cracks of the oxide layers to make them small and consequently, the microstructure of the composite coatings was rather uniform compared with the pure PEO coatings.

Anticorrosion property

The corrosion resistance of pure PEO coatings and PTFE-containing PEO coatings was evaluated by the potentiodynamic polarization curves in 3.5 wt% NaCl solution, the

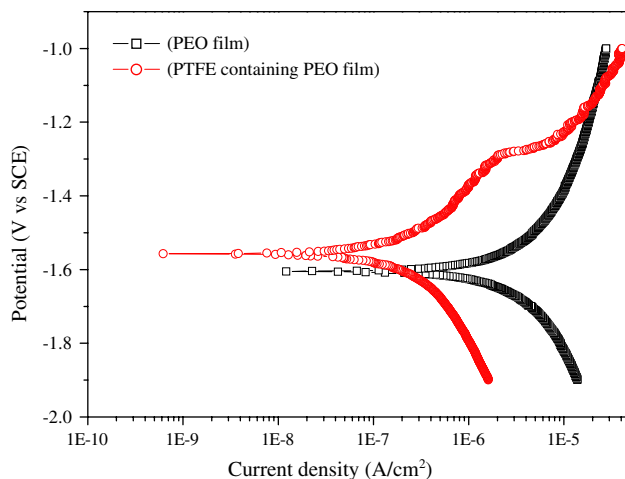


Fig. 7 Potentiodynamic polarization curves of (a) PEO coating and (b) PTFE-containing PEO coatings

Table 1 The results of potentiodynamic corrosion test of PEO coating and PTFE-containing coating in 3.5 wt% NaCl solution

	E_{corr} (V vs. SCE)	i_{corr} (A/cm ²)
PEO coating	-1.605 ± 0.006	$2.416 \pm 0.03 \times 10^{-6}$
PTFE-containing PEO coating	-1.557 ± 0.004	$2.130 \pm 0.02 \times 10^{-7}$

curves of which are shown in Fig. 7. The corrosion potential (E_{corr}) and the corrosion current density (i_{corr}) derived from the potentiodynamic polarization curves are shown in Table 1. It can clearly be observed that in NaCl solution, the corrosion potential positively increased from -1.605 V for pure PEO coatings to -1.557 V for PTFE-containing PEO coatings. Moreover, the corrosion current density of PTFE-containing PEO coatings is more than one order of magnitude lower than that of pure PEO coatings, which indicated that a better corrosion protection to Mg alloy is afforded by the PTFE-containing PEO coating when compared with pure PEO coating.

The different electrochemical corrosion behavior of the pure PEO coating and the PTFE-containing PEO coating is mainly due to their different composition and microstructures. As shown in Figs. 5a and 6a, there are many large micropores and cracks on the surface and whole layer of pure PEO coating. Therefore, with increasing of anodic potential during polarization, corrosive intermediate (Cl^-) would be rapidly transferred through the outer porous layer and reach the inner barrier layer of the PEO coating, which then increased the corrosion current density. At the same time, MgO as the main phase in the pure PEO coating, is unstable and will be subjected to progressive chemical dissolution in neutral aqueous solution [31]. All of these resulted in a limited corrosion protection of pure PEO

coatings to the Mg alloy substrate. In contrast, the PTFE-containing PEO composite coatings with small micropores and cracks (Figs. 5b and 6b) have less surface defects than pure PEO coatings. Dense oxide layer containing PTFE nanoparticles can act as a diffusion barrier and a general hindrance to corrosion at the surface of composite PEO coatings when exposed to corrosive environments, thus effectively decreasing the rapid diffusion paths for chloride ions into bulk Mg alloy substrates, which leads to a significant decrease in corrosion current density. Meanwhile, the PTFE phases are more stable than MgO phase in neutral aqueous solution. As a result, the corrosion potential of PTFE-containing PEO composite coatings is shifted to a positive potential compared to the pure PEO coating. Therefore, it can be concluded that much enhanced corrosion resistance of PTFE-containing PEO coatings in chloride containing environments can be mainly attributed to the diffusion barrier or blocking effect of dense and protective composite oxide layer on Mg alloys.

Tribological behavior of PTFE-containing PEO coatings

The typical evolution of friction coefficient with sliding time for Mg alloy substrate, pure PEO coating, and PTFE-containing PEO coating are shown in Fig. 8, respectively. For the uncoated Mg alloy substrate, the friction coefficient varies in the range of 0.2–0.4, accompanied by severe oscillation, typical of soft Mg alloy materials with adhesive wear and stick–slip tendency (curve 1 in Fig. 8). Although the friction coefficient of pure Mg alloy is low, the oscillation of friction coefficient demonstrates that the Mg alloy substrate shows poor tribological behavior without protective surface coatings. It can also be observed that the

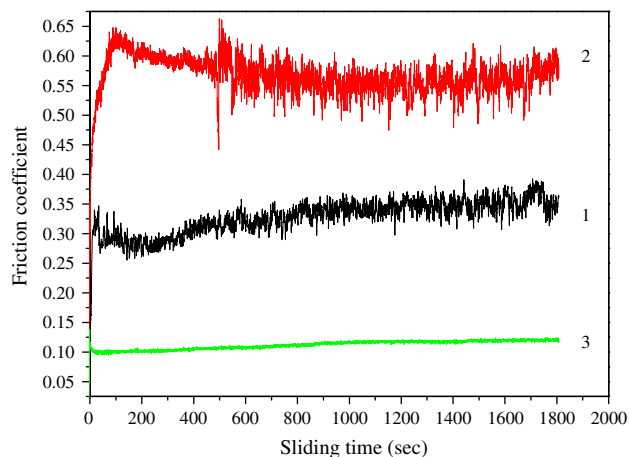


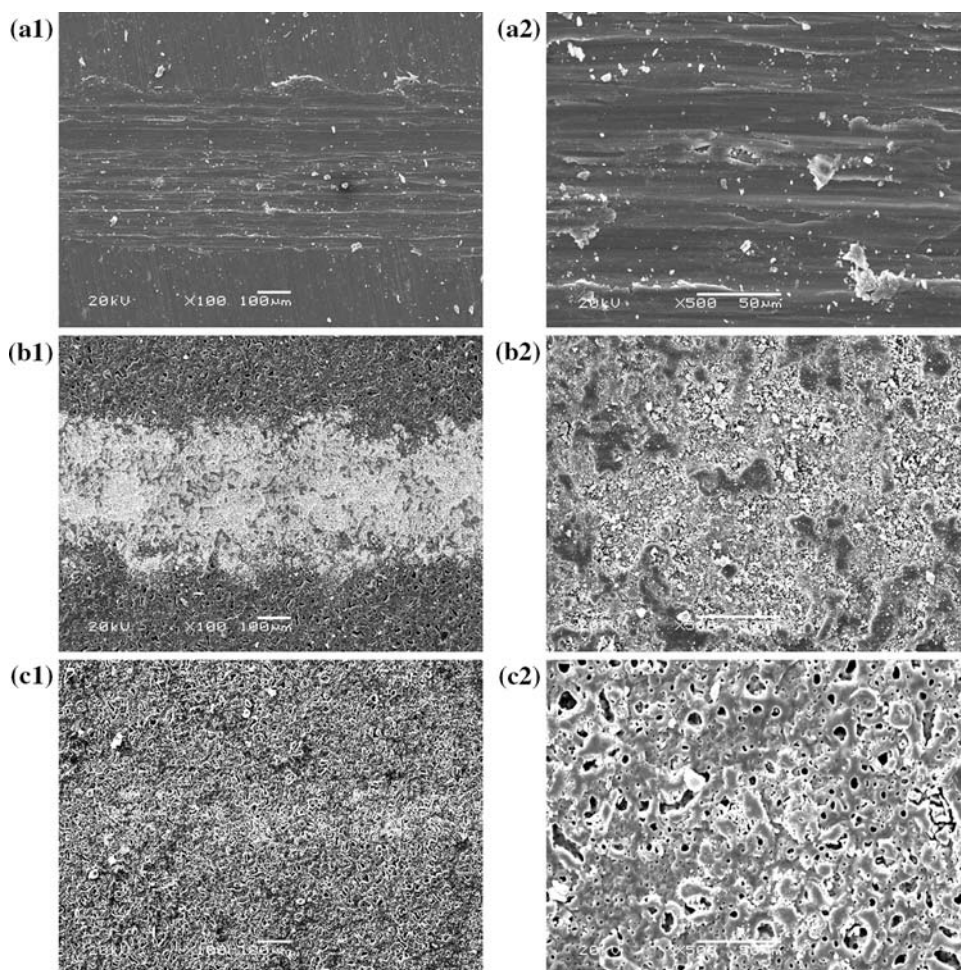
Fig. 8 Dry sliding behaviors against CCr15 steel ball for (1) Mg alloy substrate, (2) the PEO film, and (3) the PTFE-containing PEO coating

pure PEO coating shows a very high friction coefficient around 0.5–0.7 as it sliding against steel ball under unlubricated conditions (curve 2 in Fig. 8). Curve 3 in Fig. 8 shows an improved tribological behavior provided by the PTFE-containing PEO coating. The PTFE-containing PEO coating exhibited a low and stable friction coefficient (below 0.2) during the overall sliding test. It is evident that the improvement in tribological properties can be attributed to the presence of the PTFE phase in the PEO coating which acts as a solid self-lubricant during the wear test.

The improved wear resistance and remarkable reduction of friction coefficient for PTFE-containing PEO coating over Mg alloy substrate and pure PEO coatings were further confirmed by comparing the worn surface morphologies as shown in Fig. 9. It can be seen that the wear track of the Mg alloy substrate (Fig. 9a1) is broad and deep. Many grooves and scratch marks, parallel to the sliding direction, are evident on the wear track (Fig. 9a2). Such features are characteristics of abrasion wear [32, 33]. Also many scraps can be found on the wear track of pure Mg alloys. All of these indicate the Mg alloy substrate with low hardness has poor wear resistance. For the pure PEO coatings with higher

hardness than pure Mg alloys, the wear track (Fig. 9b1) is wide but not as deep as the pure Mg alloy. The coatings show severe wear characterized by a large extent of debris formation and microfractures (Fig. 9b2). However, when compared with pure Mg alloy, grooves and scratch marks cannot be found on the worn track of pure PEO coatings. So the PEO process can improve the wear resistance of Mg alloys. As shown in Fig. 9c1, the wear track of the PTFE-containing PEO coating is hard to detect, the entire worn surfaces appear quite smooth and show no evidence of appreciable material removal (Fig. 9c2). The PTFE-containing PEO coatings with higher hardness than pure Mg alloys, exhibited the lowest wear rate and friction coefficient (Fig. 8) among the three materials. This can also be attributed to the presence of the solid self-lubricating PTFE phase. Its extended chain linear molecules, $-(CF_2-CF_2)_n-$, formed low shear strength films upon its surface and mating counter-faces [34, 35]. As mentioned in other articles [36], PTFE could be easily transferred to the surface of the counter-part during the wear process, which therefore can prevent direct contact between the steel ball and the PEO coatings and act as a solid lubricant. During the dry sliding

Fig. 9 SEM micrographs of wear track after sliding tests: **a1** and **a2** for Mg alloy substrate, **b1** and **b2** for PEO film, and **c1** and **c2** for PTFE-containing PEO coating



wear process, the PTFE layer could effectively reduce the abrasion wear (as evident in Fig. 9c2) and consequently, less wear debris were generated between the contacting interfaces. This demonstrates that such nano PTFE particles can play a beneficial role in improving the dry self-lubricating performance of PEO coatings.

Hydrophobicity

Mg alloys have a number of applications in the fields of automobile and aerospace for its excellent physical and mechanical properties. Unfortunately, Mg alloys are highly susceptible to corrosion, especially in some moist service environments. According to the mechanism of corrosion protection of metals, the hydrophobic coatings with low wettability are possible to effectively prevent the water onto the substrate surface, and exhibit an excellent corrosion resistance in the wet environment. Previous studies have shown that hydrophobicity of a surface is useful for improving the corrosion resistance of Mg alloys [37]. So, under moist or water environments, hydrophobicity of Mg alloy surface is desirable for various coatings which have self cleaning and water repellent surfaces. In this case, the surface hydrophobicity of the samples showed in this work was investigated by probing the contact angle using the sessile drop measuring method. The water contact angle (CA) of the surface of pure PEO coating was measured to be in the range of $50^\circ \sim 55^\circ$, indicating that pure PEO coatings formed on Mg alloy substrates were hydrophilic. However, as shown in Fig. 10, the water CA of the PTFE-containing PEO coatings increased up to $92^\circ \sim 101^\circ$, indicating that PTFE-containing PEO coatings were hydrophobic. It can be seen that the presence of PTFE particles in PEO coatings results in the transition of the PEO coating from hydrophilic to hydrophobic. It is well known that hydrophobic surfaces require large surface roughness and low surface energy [37, 38]. As shown in Fig. 5b, the PTFE-containing PEO coatings reveal a porous microstructure and crater-like structure. Also, PTFE have excellent nonstick and hydrophobic properties [39, 40]. Therefore, in the these works, the distinguishable porous and crater-like structures developed by PEO process and the co-deposition of hydrophobic nano PTFE particles are believed to responsible for the formation of the final hydrophobicity.

Conclusions

Novel PTFE-containing PEO composite coatings with good hydrophobic properties were successfully produced on AM60B magnesium alloy using plasma electrolytic oxidation in alkaline phosphate electrolyte with addition of modified PTFE nanoparticles. The electrochemical

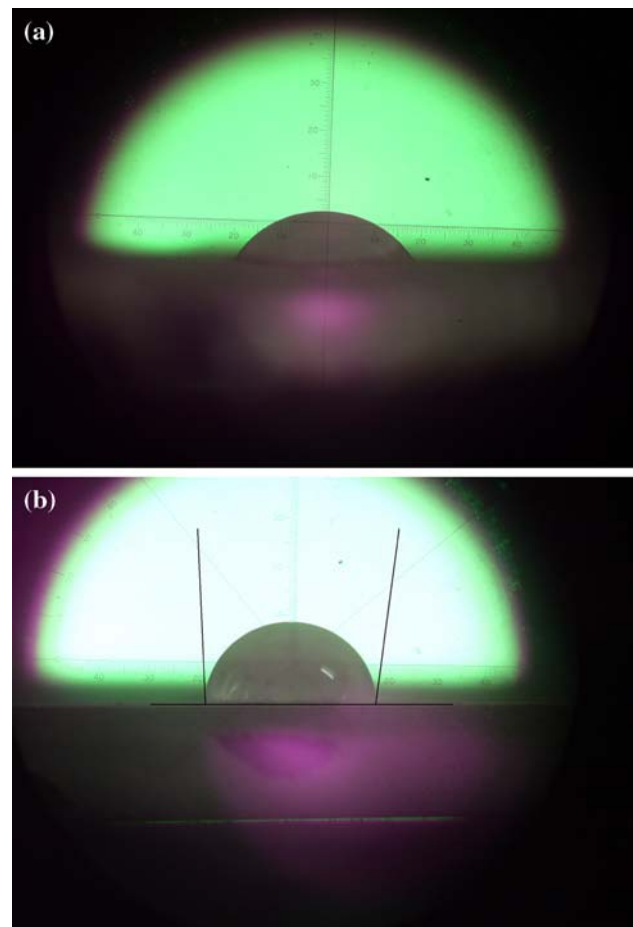


Fig. 10 Photos of the water droplet on the surface of **a** PEO coating and **b** PTFE-containing PEO coatings

corrosion property of the PTFE-containing PEO coatings was markedly superior compared to those of pure PEO coatings. Furthermore, the PTFE-containing PEO coatings exhibited improved wear resistance and lower friction coefficients compared with the pure PEO coatings and pure Mg alloys under dry sliding wear conditions. The improvement in the corrosion, tribological, and hydrophobic performance of PTFE-containing PEO coatings can be attributed to a denser and more uniform surface, solid lubrication effect of PTFE and better nonsticking properties of PTFE particles. Such multifunctional and high-performance PTFE-containing PEO coatings with superior anticorrosion, self-lubrication under dry wear conditions, and good hydrophobic properties, will be the attractive advanced materials for a wide range of functional applications.

Acknowledgements The financial support from the NSFC (Grant No.50772115), the prearranged project of General Armament Department (maintenance techniques subject) and Innovation China UK (ICUK) funding are gratefully acknowledged.

References

1. Kojina Y (2000) *Mat Sci Forum* 350–351:3
2. Kuhn A (2003) *Met Finish* 101:44
3. Song G, Atrens A, Dargusch M (1999) *Corr Sci* 41:249
4. Huang WJ, Du CH, Li ZF, Liu M, Liu WM (2006) *Wear* 260:140
5. Hiratsuka K, Enomoto A, Sasada T (1992) *Wear* 153:361
6. Blau PJ, Walukas M (2000) *Tribol Int* 33:573
7. Hoche H, Blawert C, Broszeit E, Berger C (2005) *Surf Coat Technol* 193:223
8. Ma Y, Nie X, Northwood DO, Hu H (2004) *Thin solid Films* 469–470:472
9. Guo HF, An MZ (2005) *Appl Surf Sci* 246:229
10. Yerokin AL, Shatrov A, Samsonov V, Shashkov P, Leyland A, Matthews A (2004) *Surf Coat Technol* 182:78
11. Snizhko LO, Yerokin AL, Pilkington A, Gurevina NL, Misnyankin DO, Leyland A, Matthews A (2004) *Electrochim Acta* 49:2085
12. Nie X, Leyland A, Matthews A (2000) *Surf Coat Technol* 125:407
13. Liang J, Guo BG, Tian J, Liu HW, Zhou JF, Xu T (2005) *Appl Surf Sci* 252:345
14. Hsial HY, Tsai WT (2005) *Surf Coat Technol* 190:299
15. Cai QZ, Wang LS, Wei BK, Liu QX (2006) *Surf Coat Technol* 200:3727
16. Duan HP, Du KQ, Yan CW, Wang FH (2006) *Electrochim Acta* 51:2898
17. Khaselev O, Weiss D, Yahalom J (1993) *Corros Sci* 34:1423
18. Birss V, Xia S, Yue R, Richard G, Rateick Jr (2004) *J Electrochem Soc* 151(1):B1
19. Liang J, Hu LT, Hao JC (2007) *Electrochim Acta* 52:4836
20. Liang J, Hu LT, Hao JC (2007) *Appl Surf Sci* 253:4490
21. Balaji R, Pushpavanam M, Kumar KY, Subramanian K (2006) *Surf Coat Technol* 201:3205
22. Liang J, Guo BG, Tian J, Liu HW, Zhou JF, Liu WM, Xu T (2005) *Surf Coat Technol* 199:121
23. Ger M (2004) *Mater Chem Phys* 87:67
24. Berkh O, Eskin S, Zahavi J (1994) *Plat Surf Fin* 81:62
25. Hovestad A, Janssen LJJ (1995) *J Appl Electrochem* 25:519
26. Wang LP, Gao Y, Liu HW, Xue QJ, Xu T (2005) *Surf Coat Technol* 191:1
27. Ger MD, Hwang BJ (2002) *Mater Chem Phys* 76:38
28. Moulder JF, Stickle WF, Sobol PE, Jill C (eds) (1995) *Handbook of X-ray photoelectron spectroscopy*. Physical Electronic Inc. Press, Minnesota
29. Zozulin AJ, Bartak DE (1994) *Met Finish* 92(3):39
30. Sharma AK, Uma RR, Malek A, Acharya KSN, Muddu M, Kumar S (1996) *Met Finish* 94:16
31. Zhang Y, Yan C, Wang F, Li W (2005) *Corros Sci* 47:2816
32. Hokkirigawa K, Kato K (1981) *Tribol Int* 21:51
33. Lim CYH, Lim SC, Gupta M (2003) *Wear* 255:629
34. Tanaka K, Uchiyama Y, Toyoka S (1973) *Wear* 23:153
35. Blanchet TA, Peng Y, Nablo SV (1998) *Tribol Lett* 4:87
36. Yang E-L, Hirvonen J-P (1991) *Wear* 146:367
37. Li WP, Zhu LQ, Liu HC (2006) *Surf Coat Technol* 201:2573
38. Liang J, Guo ZG, Fang J, Hao JC (2007) *Chem Lett* 36:416
39. Huang F, Wei Q, Liu Y et al (2007) *J Mater Sci* 42:8025. doi:[10.1007/s10853-007-1580-3](https://doi.org/10.1007/s10853-007-1580-3)
40. Pascual M, Balart R, Calvo O et al (2008) *J Mater Sci* 43:4901. doi:[10.1007/s10853-008-2712-0](https://doi.org/10.1007/s10853-008-2712-0)